HYDROLOGICAL PROCESSES
Hydrol. Process. **20**, 3207–3225 (2006)
Published online in Wiley InterScience
(www.interscience.wiley.com) DOI: 10.1002/hyp.6328

Riparian ecohydrology: Regulation of water flux from the ground to the atmosphere in the Middle Rio Grande, New Mexico

James R. Cleverly,[1]* Clifford N. Dahm,[1] James R. Thibault,[1] Dianne E. McDonnell[1,2] and Julie E. Allred Coonrod[2]

[1] *Department of Biology, MSC03 2020, 1 University of New Mexico, Albuquerque, New Mexico, 87131-0001, USA*
[2] *Department of Civil Engineering, MSC01 1070, 1 University of New Mexico, Albuquerque, New Mexico, 87131-0001, USA*

Abstract:

During the previous decade, the south-western United States has faced declining water resources and escalating forest fires due to long-term regional drought. Competing demands for water resources require a careful accounting of the basin water budget. Water lost to the atmosphere through riparian evapotranspiration (ET) is believed to rank in the top third of water budget depletions. To better manage depletions in a large river system, patterns of riparian ET must be better understood. This paper provides a general overview of the ecological, hydrological, and atmospheric issues surrounding riparian ET in the Middle Rio Grande (MRG) of New Mexico. Long-term measurements of ET, water table depth, and micro-meteorological conditions have been made at sites dominated by native cottonwood (*Populus deltoides*) forests and non-native saltcedar (*Tamarix chinensis*) thickets along the MRG. Over periods longer than one week, groundwater and leaf area index (LAI) dynamics relate well with ET rates. Evapotranspiration from *P. deltoides* forests was unaffected by annual drought conditions in much of the MRG where the water table is maintained within 3 m of the surface. Evapotranspiration from a dense *Tamarix chinensis* thicket did not decline with increasing groundwater depth; instead, ET increased by 50%, from 6 mm/day to 9 mm/day, as the water table receded at nearly 7 cm/day. Leaf area index of the *T. chinensis* thicket, likewise, increased during groundwater decline. Leaf area index can be manipulated as well following removal of non-native species. When *T. chinensis* and non-native Russian olive (*Elaeagnus angustifolia*) were removed from a *P. deltoides* understory, water salvaged through reduced ET was 26 cm/yr in relation to ET measured at reference sites. To investigate correlates to short-term variations in ET, stepwise multiple linear regression was used to evaluate atmospheric conditions under which ET is elevated or depressed. At the *P. deltoides*-dominated sites, ET anomalies were positively correlated to net radiation (R_n) and negatively correlated to sensible heat flux (H), cross-corridor wind speed (v), and along-corridor wind speed (u) ($r^2 = 0{\cdot}54$). At the *T. chinensis*-dominated sites, ET anomalies were positively correlated with R_n, u, the friction coefficient (u_*), and vapour pressure deficit (VPD) and were negatively correlated to surface humidity scale (q_*), daily high and low temperature, H, and precipitation ($r^2 = 0{\cdot}66$). Both *Tamarix* and *Populus* can transpire prodigious quantities of water when conditions are favourable. In the MRG, *T. chinensis* is preferentially found where summer flooding and cold air drainage occurs, and *P. deltoides* is preferentially located in areas with shallow groundwater within 2 m of the surface. Copyright © 2006 John Wiley & Sons, Ltd.

KEY WORDS eddy covariance; depth to groundwater; phreatophytes; Rio Grande cottonwood; saltcedar; Russian olive; transpiration; evapotranspiration; leaf area index; micrometeorology; floodplain

Received 9 March 2005; Accepted 1 March 2006

INTRODUCTION

Riparian habitats worldwide are emerging as intense political, economic, social, and ecological battlegrounds over limited water resources (Zube and Simcox, 1987; Jackson *et al.*, 2001). In arid and semi-arid regions,

* Correspondence to: James R. Cleverly, Department of Biology, MSC03 2020, 1 University of New Mexico, Albuquerque, New Mexico, 87131-0001, USA. E-mail: cleverly@sevilleta.unm.edu

freshwater resources are concentrated along riparian corridors. These oases support high biodiversity, enhanced ecosystem productivity, and agricultural, municipal, and industrial demands for water (Malanson, 1995). The focus of human activities along rivers changes stream hydrology and ecology: perennial streams become ephemeral, diversions lower the water table, and plant stress leads to loss of native vegetation and shifts in species composition from native to non-native species (Medina, 1990; Smith *et al*., 1991).

Increasing density of non-native species, along with declining ecological importance of native species, has been described in nearly all river systems throughout the western United States (Howe and Chancellor, 1983; Snyder and Miller, 1993; Di Tomaso, 1998; Pataki *et al*., 2005; Shafroth *et al*., 2005). The two most common non-native plants in western U.S. river corridors are *Tamarix* L. (saltcedar), and *Elaeagnus angustifolia* (Russian olive) (Friedman *et al*., 2005). *Tamarix* spp. are primarily *Tamarix ramosissima* and closely related *Tamarix chinensis* and hereafter referred to as *Tamarix*. Both *Tamarix* and *E. angustifolia* originated in Eurasia, and they represent the third and fourth most common species found in western U.S. riparian areas, after *Salix exigua* (sandbar or coyote willow) and *Populus deltoides* (plains cottonwood) (Friedman *et al*., 2005). The range of *E. angustifolia* is still expanding, while *Tamarix* dominance appears to be reaching an equilibrium in which expansion of *Tamarix* in some locations is balanced by loss of *Tamarix* in other locations (Friedman *et al*., 2005). Examples of native species maintaining or recovering community dominance have been observed in the Rio Grande and Colorado River systems (Snyder and Miller, 1993; Cleverly *et al*., 1997; Nagler *et al*., 2005b).

Riparian ecosystems that are prone to invasion by non-native species are characterized by greater disturbance frequency and intensity, deeper water tables, greater fluctuation of water table depth, greater surface salinity, and flood timing outside the regeneration window for native species (Smith *et al*., 1991; Busch and Smith, 1993; Busch and Smith, 1995; Planty-Tabacchi *et al*., 1996; Lite and Stromberg, 2005; Tiegs *et al*., 2005). Characteristics of *Tamarix* that contribute to its ecological success include fruit production extending across the growing season; greater reproductive output; tolerance of heat, salinity, drought, and flooding stresses; regeneration following fire; induced sediment accretion with resultant deepening of the water table; surface soil salinization; and profligate transpiration from both groundwater and soil water sources (Warren and Turner, 1975; Busch *et al*., 1992; Sala *et al*., 1996; Di Tomaso, 1998; Cleverly *et al*., 2002). Extensive reviews of *Tamarix* and *E. angustifolia* invasion ecology have been provided by Di Tomaso (1998); Katz and Shafroth (2003), respectively.

The potential for non-native vegetation to remove prolific quantities of water from the ground is of serious concern to water resource managers, although a great deal of controversy continues to exist regarding water use by *Tamarix* (Hughes, 1993; Shafroth *et al*., 2005). This controversy is driven by estimates of *Tamarix* water use that vary wildly, depending upon habitat and upon how water use is measured or estimated (Hughes, 1993; Cleverly *et al*., 2002; Shafroth *et al*., 2005). This paper will present a case study in riparian evapotranspiration (ET) along the Middle Rio Grande (MRG), New Mexico, USA. There were two main objectives of this study: (1) to determine the relative evapotranspirational water losses from non-native and native riparian species under a range of natural environmental variations (Cleverly *et al*., 2002; Dahm *et al*., 2002); and (2) to investigate short- and long-term patterns of variability in measured ET for evaluating potential water salvage for riparian restoration and vegetation management (Molles *et al*., 1998; Shafroth *et al*., 2005; Newman *et al*., 2006).

EVAPOTRANSPIRATION

ET is the process by which water is transported from the surface to the atmosphere as water vapour. ET is the combined evaporation from soil, open water, and ice surfaces, along with transpiration from vegetation. In riparian areas, the presence of shallow groundwater provides an ample water supply, permitting greater annual ET rates than precipitation (PPT) (Dahm *et al*., 2002; Huxman *et al*., 2005). Because ET from most ecosystems within a large basin is limited by PPT, riparian corridors exist as a hot spot of water loss to the

DOI: 10.1002/hyp

atmosphere within large arid- and semi-arid basins (Devitt *et al*., 1998; Kurc and Small, 2004; Huxman *et al*., 2005). Soil evaporation is negligible under riparian canopies owing to attenuation of radiation by vegetation (Saugier and Katerji, 1991; Wilson *et al*., 2001). Riparian ecosystems are characterized by a high transpiration to ET ratio in the south-western United States, especially where groundwater is near the surface (Scott *et al*., 2003; Kurc and Small, 2004; Huxman *et al*., 2005; Newman *et al*., 2006).

Water budgeting has long been used to integrate large-scale surface water and groundwater dynamics. In large river systems, uncertainty in estimating the numerous pathways through which water can enter or leave a basin requires the use of the best 'guesses' for depletions such as riparian ET, groundwater recharge, and surface water–groundwater interactions (Scott *et al*., 2000; Cleverly *et al*., 2002; Dahm *et al*., 2002). Of these depletions, ET from phreatophytes such as *P. deltoides* and *S. exigua* represents most of the 20–50% of total long-term water budget depletions that are ascribed to natural vegetation (Scott *et al*., 2000; Dahm *et al*., 2002).

Many methods used for estimating ET are based upon the application of the energy balance, or conservation of incoming and outgoing energy. Under steady state conditions, and assuming a closed system, energy entering the canopy will be balanced by energy leaving the canopy:

$$R_n = \lambda E + H + G \tag{1}$$

where R_n is the net radiation, λE is latent heat flux, H is sensible heat flux, and G is the ground heat flux (W m^{-2}). Net radiation is the difference between downward- and upward-directed radiative energy flux:

$$R_n = (Q_{L\downarrow} + Q_{S\downarrow}) - (Q_{L\uparrow} + Q_{S\uparrow}) \tag{2}$$

where Q is radiative energy flux, L and S represent long-wave (i.e. thermal) and short-wave (i.e. solar) radiation, respectively. The direction of the arrow indicates whether radiation is directed down into the canopy or up away from the canopy. By convention, R_n is positive when directed toward the surface, and the remaining terms are positive when directed away from the surface. Latent heat flux represents the energy absorbed or released when water changes phase. Ground heat flux is the heat conducted through the soil surface, and H is the convective energy flux generated by atmospheric temperature gradients.

The Bowen ratio energy balance (BREB) method, for example, has been used for decades to estimate *Tamarix* ET (Gay and Fritschen, 1979; Devitt *et al*., 1998). This method utilizes measurements of R_n, G, and the Bowen ratio, β, to determine λE:

$$\beta = \frac{H}{\lambda E} = \frac{C_P}{\lambda \varepsilon} \frac{(T_2 - T_1)}{(\chi_2 - \chi_1)} \tag{3}$$

where C_p is the heat capacity of air, λ is the latent heat of vapourization, T is temperature, ε is the ratio of the molecular weights of water and dry air, and χ is the mole fraction of the partial pressure of water vapour. Temperature and humidity are each measured at two heights above the canopy where the subscript 2 refers to the upper measurement. Latent heat flux is determined as the residual of the energy balance (Equation 1):

$$\lambda E = \frac{R_n - G}{1 + \beta} \tag{4}$$

Bowen ratio energy balance methods have been applied successfully in wetlands with adequate fetch and a homogeneous canopy (Drexler *et al*., 2004). Even when these conditions are met, however, energy balance estimates of ET can be confounded by sensible heat advection, which is the horizontal movement of momentum, energy, or other scalar quantities across a heterogeneous landscape (Itier *et al*., 1994; McAneney *et al*., 1994; Devitt *et al*., 1998; Cooper *et al*., 2000; Drexler *et al*., 2004). Advection occurs when wet surfaces, such as wetlands or irrigated ecosystems, are located adjacent to dry surfaces such as arid and semi-arid rangeland ecosystems. Sensible heat advection into riparian forests is most easily identified when the evaporative fraction, which is the ratio λE: R_n, is greater than unity (Devitt *et al*., 1998).

DOI: 10.1002/hyp

Three-dimensional sonic eddy covariance (3SEC) is the benchmark method for measuring fluxes over tall vegetation, under advection, and in complex terrain (Brunet *et al*., 1994; McAneney *et al*., 1994; Simpson *et al*., 1998; Drexler *et al*., 2004). One advantage of the 3SEC system is that ET is measured directly, rather than estimated as the residual of the energy balance (Equation 4). Thus, 3SEC is the only method that provides the means of estimating energy balance closure error as a self-check for accuracy (Twine *et al*., 2000; Drexler *et al*., 2004).

The core instruments in 3SEC systems are a 3D sonic anemometer to measure wind speed in three dimensions, a krypton hygrometer or an infrared gas analyser (IRGA) to measure humidity, a thermocouple with a very exact fine-wire junction (0·0127 mm diameter type E chromel–constantan) to avoid signal retention in high-frequency measurements, and an IRGA to measure CO_2 concentration. Each of these instruments make measurements at a frequency determined through spectral decomposition of sample time series taken at 20 Hz. A sampling frequency is chosen in the high-frequency spectral gap, usually between 5 and 20 Hz (Stull, 1988).

Latent heat flux (λE), or the heat absorbed by evaporation, is computed from these measurements as a function of the covariance between vertical wind speed and humidity:

$$\lambda E = \lambda \overline{w'q'} = \lambda \sum_{i=1}^{n} \frac{(w_i - \overline{w})(q_i - \overline{q})}{n} = \lambda \mathrm{Cov}(wq) = \lambda \rho_w \mathrm{ET} \tag{5}$$

where λ is the latent heat of vapourization, w' is the instantaneous deviation from mean vertical wind speed (i.e. $w' = w_\mathrm{i} - \overline{w}$), ρ_w is the density of water, and q' is the instantaneous deviation from average water vapour density. The period for averaging, n, is chosen from balancing the spectral gap with minimizing trending in very low frequencies. Covariance periods are typically 15–40 min long. Sensible heat flux (H, heat transfer due to vertical atmospheric temperature gradients) is computed likewise as a function of the covariance between vertical wind speed and temperature:

$$H = C_p \rho_a \overline{w'T'} = C_p \rho_a \sum_{i=1}^{n} \frac{(w_i - \overline{w})(T_i - \overline{T})}{n} = C_p \rho_a \mathrm{Cov}(wT) \tag{6}$$

where ρ_a is density of wet air, and T' is the instantaneous deviation of temperature from mean air temperature.

Before ET is computed from LE, various standard corrections are applied to incorporate the physical realities within which these measurements are made. These corrections include coordinate rotation to align the wind vector with the sonic anemometer (Wesely, 1970), corrections developed from frequency response relationships that incorporate sensor line averaging and separation (Massman, 2000; Massman, 2001), corrections to account for flux effects on vapour density measurements as opposed to mixing ratio measurements (Webb *et al*., 1980), and krypton hygrometer oxygen and second-order humidity effects on vapour density measurements. Lastly, closure of the energy balance is forced into thermodynamic equilibrium by adding closure energy into H and λE in relation to the measured Bowen ratio (Twine *et al*., 2000; Cleverly *et al*., 2002).

Measurement of turbulent fluxes via 3SEC involves measuring flux variables from a tower or an aircraft. When measurements are made from a tower, the minimum spacing between a canopy and the sensors is dictated by the necessity to make measurements above the roughness sublayer. The top of the roughness sublayer is equal to the distance of the aerodynamic roughness length, z_0, above the canopy, h_c (Nakamura and Mahrt, 2001). The upper limit for sensor placement in riparian corridors is chosen to remain below the top of the surface layer and to minimize the measurement footprint (Cooper *et al*., 2000; Cooper *et al*., 2003b). The top of the surface layer is defined in terms of Monin–Obukhov theory, which describes the physics of the atmospheric surface layer (Stull, 1988). Atmospheric stability imposed by advection is associated with vertical thermal stratification and compression of the surface layer to the lower few meters above the canopy (Cooper *et al*., 2003b).

The planetary boundary layer is that lower portion of the atmosphere where turbulence dominates vertical transport and friction creates a strong drag on near-surface winds. The surface layer makes up the bottom

DOI: 10.1002/hyp

10% of the boundary layer (Stull, 1988), where surface drag creates a near-logarithmic wind speed profile. The vertical gradient in horizontal wind speed causes deformation of the air column and generates turbulence that can be characterized by Reynolds stress, τ_{Reynolds}, which is equal to the total vertical flux of horizontal momentum in the surface layer (Stull, 1988):

$$|\tau_{\text{Reynolds}}| = \overline{\rho}[(\overline{u'w'})^2 + (\overline{v'w'})^2]^{1/2} \tag{7}$$

where ρ is density of air, and u, v, and w are orthogonal wind speeds in two horizontal and one vertical dimensions, respectively. The velocity scale across which Reynolds stresses are propagated is the friction coefficient, u_* (Stull, 1988):

$$u_* = \frac{|\tau_{\text{Reynolds}}|}{\rho} = \left[(\overline{u'w'})^2 + (\overline{v'w'})^2\right]^{1/2} \tag{8}$$

The friction coefficient is important in describing the magnitude of turbulence in the surface layer, and that prominence is central to the body of the relationships known as Monin–Obukhov (M–O) similarity theory. M–O similarity theory, also known as surface layer similarity theory, is a body of empirical relationships that characterize turbulence in the surface layer. Other M–O scales useful for characterizing the surface layer include the humidity scale, ${q_*}^{\text{SL}}$, the temperature scale, ${\theta_*}^{\text{SL}}$, and the Obukhov length, L (Stull, 1988):

$$q_* = \frac{-\overline{w'q'}}{u_*} \tag{9}$$

$$\theta_* = \frac{-\overline{w'T'}}{u_*} \tag{10}$$

$$L = \frac{-\overline{T}u_*^2}{kg\theta_*} \tag{11}$$

where k is von Kármán's constant and g is the acceleration due to gravity. When L is zero, the surface layer is neutrally stratified. When negative, the surface layer is unstably stratified, and the temperature profile in the surface layer is stable when L is positive. The Semi-Arid Land-Surface-Atmosphere (SALSA) program, which brought together eddy covariance and Lidar (light detection and ranging) technologies to measure ET in the San Pedro River of Arizona, generated the first detailed characterization of the turbulent boundary layer in a riparian corridor (Cooper *et al*., 2000; Goodrich *et al*., 2000; Kao *et al*., 2000; Scott *et al*., 2000).

The measurement footprint represents the upwind distance that is incorporated into measurements made by instruments on the tower. The footprint increases with height above the canopy and with wind speed (Rannik *et al*., 2000). In riparian forests along the MRG and the San Pedro River, the footprint for sensors mounted 2·5 m above *Tamarix* may be as little as 40–60 m under ideal conditions, or up to 200 m over *Populus fremontii* (Fremont cottonwood) and *Sporobolus wrightii* (sacaton grass) (Cooper *et al*., 2000; Cooper *et al*., 2003b).

THE MIDDLE RIO GRANDE

The MRG is located in New Mexico, USA, and is defined to coincide with the New Mexico delivery obligation supply index gauges near Otowi NM and at Elephant Butte Dam, set forth in the Rio Grande compact (revised 1948). The MRG has three tributaries within the basin: the Jemez River, the Rio Puerco, and the Rio Salado (Figure 1). The Rio Puerco and Rio Salado contribute flood flow to the MRG during summer monsoon periods. Three dams divert water from the Rio Grande to support irrigated agriculture (Figure 1): the Angostura diversion dam downstream of the confluence between the Rio Grande and the Jemez River, the Isleta pueblo diversion dam downstream of Albuquerque NM, and the San Acacia diversion dam downstream of the confluence of the Rio Grande with the Rio Salado. Three more dams create reservoirs in the MRG

DOI: 10.1002/hyp

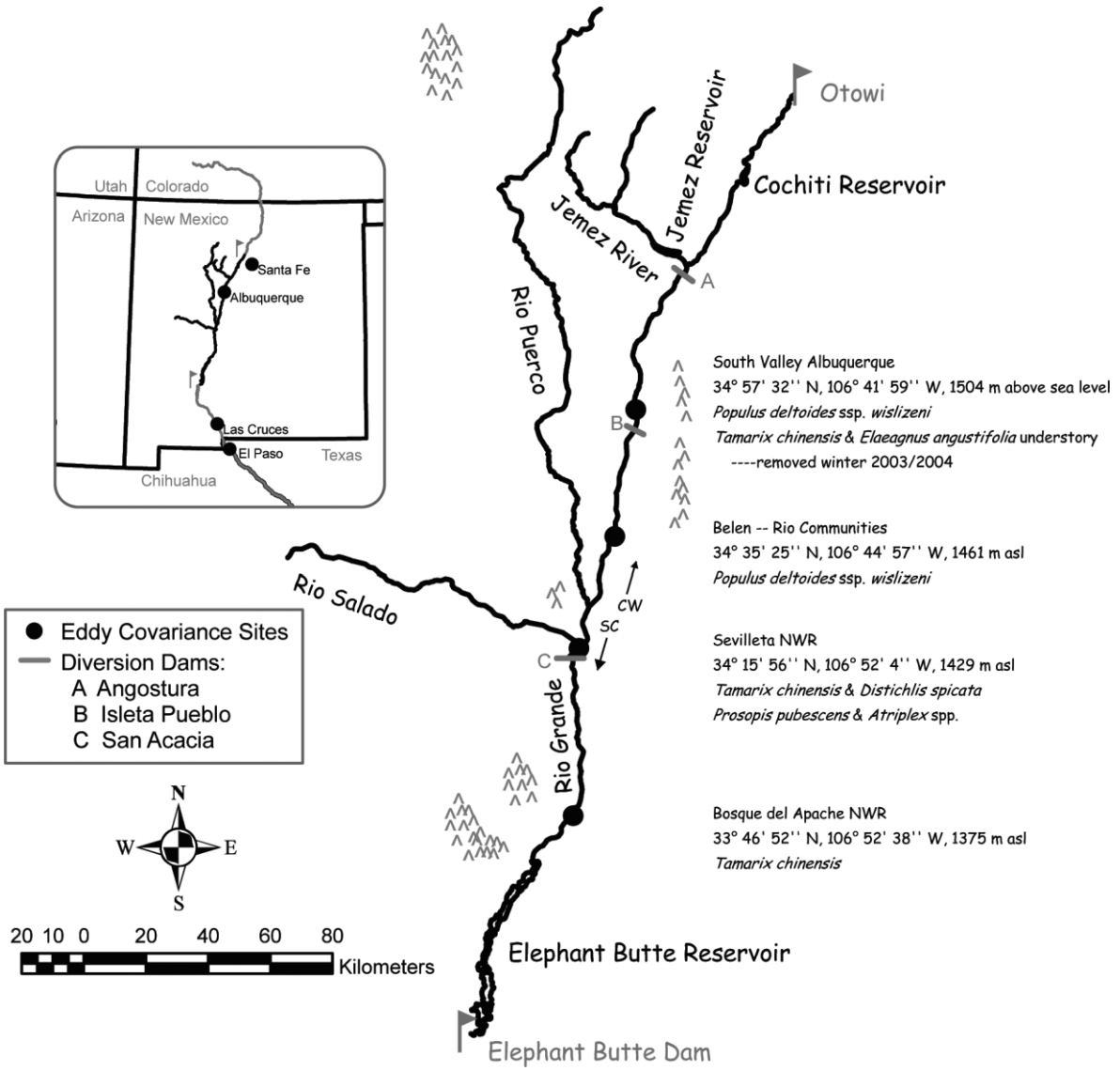

Figure 1. Map of the MRG in New Mexico, USA. Locations of local cities are marked in the inset map. The MRG, originating in Otowi NM and discharging from Elephant Butte Reservoir, is dominated in the north by *P. deltoides* ssp. *wislizeni* (Rio Grande cottonwood) and by *Tamarix chinensis* (saltcedar) in the southern reaches. Locations of nearby mountain ranges are illustrated, along with diversion dams, reservoirs, and tributaries. Four sites with tower-based eddy covariance systems are listed along with site locations and local riparian vegetation

basin (Figure 1): at Cochiti Pueblo, at Jemez Pueblo, and at Elephant Butte near Truth or Consequences, NM. Elephant Butte Lake is the only reservoir with significant storage capacity, and the remaining reservoirs are principally operated for flood control. Mountainous terrain, identified in a 100-m resolution digital elevation model, was identified in the northern and southern portions of the MRG, while the Albuquerque and Belen reaches are overlooked by mesas (Figure 1).

Flood control was promoted by the addition of riverside drains and levees during the early to mid twentieth century. Exceptionally high flows in the river are contained within undeveloped riparian zones through the

DOI: 10.1002/hyp

construction of levees. Adjacent to this levee system are drains that were excavated to an elevation below river channel bottom. These drains were placed to generate a hydrologic gradient away from the valley bottom, thus curtailing flooding beyond the levees. Excess water applied in irrigation is leached into the drain system.

One further significant hydrologic feature is the City of Albuquerque's wastewater reclamation plant. This plant was originally established in 1962 and contributes *ca* 40% of the tributary inflow to the MRG, not including trans-basin transfers and tributary inflow in the upper Rio Grande basin above Otowi (Cleverly *et al*., 2002; Dahm *et al*., 2002). The origin of this water is the deep paleoaquifer, from where it is pumped up at stations throughout the Albuquerque sub basin, providing long-term water resources to the MRG.

In arid and semi-arid regions, water loss to the atmosphere in riparian corridors dominate basin water budgets, representing well over 90% of MRG depletions due to open water evaporation, soil evaporation, transpiration, and irrigated agriculture (Cleverly *et al*., 2002; Dahm *et al*., 2002). ET from riparian vegetation has been estimated to represent 30% of the total depletions in the MRG water budget.

Since the early twentieth century, riparian vegetation density and cover has been slowly increasing in all reaches of the Upper and MRG owing to anthropogenic modifications of the MRG's hydrology (Everitt, 1998). On the Rio Grande, upstream of its confluence with the Rio Puerco, *P. deltoides* cover has been increasing (Snyder and Miller, 1993). By the 1960s, woody vegetation cover reached a maximum in the MRG at Albuquerque, where *P. deltoides* represented nearly all the 75% ground cover (Campbell and Dick-Peddie, 1964). Downstream of the Rio Grande's confluence with the Rio Puerco, *Tamarix* thickets and woodlands have expanded the area covered by woody vegetation while *P. deltoides* cover has decreased (Howe and Knopf, 1991; Everitt, 1998) (Figure 1).

Currently, dense monocultures of non-native *T. chinensis* Lour. (saltcedar) dominate the floodplain downstream of the Rio Grande's confluence with the Rio Puerco (Figure 1). These thickets cover 100% of the land surface between riverside levees. In contrast, reaches of the Rio Grande upstream of the Rio Puerco's confluence are fully covered by dense *P. deltoides* ssp. *wislizeni* (S. Watson) Eckenw. (Rio Grande cottonwood) forests. In many locations, these *P. deltoides* forests include a dense understory of non-native species, predominately *E. angustifolia* L. (Russian olive) and *Tamarix* (Figure 1).

STUDY AREA AND METHODS

Four sites were chosen in 1998. Two locations of large extent were identified in *P. deltoides* forests, one with a short (i.e. less than 3 years) interflood interval, and the other with a long (i.e. greater than 40 years) interflood interval. Two *Tamarix* stands were likewise chosen with short and long interflood intervals (Molles *et al*., 1998). The northernmost site, located in the south valley of Albuquerque, New Mexico, hosted a sparse *P. deltoides* forest (122 trees ha^{-1}) and a very dense understory thicket of *Tamarix* and *E. angustifolia* until 2004, when the understory was removed as part of a citywide restoration project (Figure 1). The other *P. deltoides*-dominated site, located near the towns of Belen and Rio Communities NM, regularly receives flooding and supports a high-density forest (278 trees ha^{-1}) with predominantly native understory species. In November 1999, a 25-m tower was established to measure ET in each of these *P. deltoides* forests.

The northernmost *Tamarix*-dominated site is located at the Sevilleta National Wildlife Refuge (NWR), home of the Sevilleta Long Term Ecological Research (LTER) program. This site is located between the confluence of the Rio Salado and the San Acacia diversion structure, and the vegetation is a mosaic of *Tamarix* thickets, *D. spicata* meadows, and various halophytes like *Prosopis pubescens* Benth. (screwbean mesquite) and *Atriplex* L. spp (saltbush). A 10-m eddy covariance tower was established at this site in March 1999. The second *Tamarix*-dominated site is located at Bosque del Apache (BDA) NWR. This site is frequently flooded and contains a dense (15 000 shrubs ha^{-1}), monospecific *Tamarix* thicket. The U.S. Bureau of Reclamation and New Mexico State University established a 15-m tower in this thicket in 1998.

Three-dimensional eddy covariance systems were mounted on the towers, 2–2·5 m above the canopy (Cleverly *et al*., 2002; Dahm *et al*., 2002). The measurement period was 10 Hz and the covariance period was

DOI: 10.1002/hyp

30 min. Additional energy flux measurements were made at 1 Hz and averaged over 30 min. Net radiation was measured using annually cross-calibrated REBS Q7·1 net radiometers. Ground heat flux was measured using REBS ground heat flux plates, corrected for heat storage in the 8 cm of soil above the plate using Campbell Scientific, Inc. (CSI) soil temperature thermocouples (TCAV) and soil water content (CSI CS616) measurements. Average energy balance closure for all systems in all years, determined on a daily basis, was 78%, and the Bowen ratio was near zero during the growing season (Cleverly *et al*., 2002). These are values typical of eddy covariance and riparian corridors, respectively (Devitt *et al*., 1998; Wilson *et al*., 2002).

Complementary measurements made from each tower included standard weather station conditions (i.e. precipitation, temperature, relative humidity, horizontal wind speed and direction; Campbell Scientific, Inc., Logan, UT). Measurements of vapour pressure were used to calculate vapour pressure deficit (VPD) as the difference between atmospheric vapour pressure (e_a, kPa) and saturation vapour pressure (e_s, kPa). This difference represents the vapour pressure gradient from the saturated tissues within a leaf to the free atmosphere.

A network of five shallow groundwater wells was placed at each site, with one well near the tower and four additional wells in the four cardinal directions 40 m from the central well. Three of the wells at each of the sites were equipped with automated pressure transducers, measuring water level every 30 min (EEI, Las Cruces, NM). In 2003, all five wells at each site were instrumented with pressure transducers, with a subset of those also measuring groundwater temperature (Solinst Canada Ltd, Georgetown, Ontario).

Plant area index (PAI), which is the projected area of leaves and stems per unit ground area, was measured from below relatively undisturbed vegetation adjacent to each of the five groundwater wells using the LAI2000 (Li-cor, Inc., Lincoln, NE). Two measurements above the canopy and five measurements below the canopy were made in each plot. The first and second plots were double-sampled to track changes in measured PAI with changing light conditions. Measurements were made monthly during the growing season, as well as once during the winter of 2001–2002 to estimate stem area index (SAI). Retention by *P. deltoides* of senescent leaves through the winter confounds the winter measurement from *P. deltoides* forests. Measurements were made either during 45 min between sundown and dark or, weather permitting, under cloud cover. Measurements of clear sky conditions were made from a ladder or from the tower at *Tamarix* sites and from the nearby levee at *P. deltoides* sites because the vegetation is taller than 20 m.

Plant area index is equal to the sum of the projected leaf area index LAI and SAI, less the area of overlap between stems and leaves. In broadleaf species, such as *P. deltoides*, the overlap between stem area and leaf area is the same as SAI, thus PAI equals projected LAI (Gower and Norman, 1991; Chen and Black, 1992; Chen and Cihlar, 1995; Chen and Cihlar, 1996). Incorporation of leaf geometry was considered in three leaf types: broadleaf tree (i.e. *P. deltoides* and *E. angustifolia*), flat leaf shrubs (i.e. *S. exigua*), and cylindrically leaved shrubs (i.e. *Tamarix*). Leaf area index of the three-dimensional leaf surface was determined for each leaf type as follows:

$$LAI(broadleaf)_{total} = 2 \times PAI \tag{12}$$

$$LAI(flat)_{total} = 2 \times (PAI - SAI) \tag{13}$$

$$LAI(cylindrical)_{total} = \pi \times (PAI - SAI) \tag{14}$$

Stepwise multiple linear regression (proc GLM, Statistical Analysis Software, SAS Institute, Inc., Cary, NC) was used to evaluate the effect of micro-meteorological conditions on daily ET rates (Nagler *et al*., 2005a). A suite of micro-meteorological variables was chosen for the analysis representing surface layer aerodynamics, energy fluxes, and standard weather phenomena. Because temporal autocorrelation in micro-meteorological time series data violate the critical regression assumption of independent and identically distributed (i.i.d.) measurements, anomaly analysis was chosen to resample the time series and thereby eliminate i.i.d. restrictions (Higgins *et al*., 1997). ET anomalies are identified as having a value greater or lesser than one standard deviation from average, computed as the 9-day running average, $\overline{ET_{9-day}}$. These $n = 43 \pm 3$ anomalies per

DOI: 10.1002/hyp

year from each tower are then used as the dependent variable in both forward and reverse steps. This analysis indicates which micro-meteorological conditions are related to driving daily ET above or below the long-term average.

DROUGHT AND GROUNDWATER (SLOW DYNAMICS)

In the year 2000, the *P. deltoides* forest with a non-native understory had the highest annual ET (Albuquerque) (Table I). The lowest ET in every year was generated by the xeroriparian *Tamarix* woodland at the Sevilleta NWR (Table I). This xeroriparian *Tamarix* woodland was also distinguished by having the highest ET : LAI ratio of all the sites (Table I). The vegetation in this location is predominantly a mosaic of *Tamarix* and *D. spicata. P. pubescens* (screwbean mesquite) and *Atriplex* spp. are also present at the Sevilleta site. Of the sites with intermediate annual ET, monospecific *Tamarix* (BDA NWR) lost more water through ET than the *P. deltoides* forest containing a mostly native understory (Belen—Rio Communities) (Table I). Average annual precipitation is 20–31 cm in the MRG (Dahm *et al*., 2002), and the ET : PPT ratio was greater than unity at all sites in all years.

Removal of non-native species from the understory of a *P. deltoides* forest had a modest effect on forest ET. Evapotranspiration decreased by 9% following removal of non-native species between 2003 and 2004 (Table I). However, ET at both the *Tamarix*-dominated sites increased in 2004 by 12% over the 2003 ET (Table I). Assuming that the *Tamarix* sites represent the reference conditions for ET water loss in the basin, the net decrease in ET due to removal of non-native species is 21%, a savings of 26 cm in the first year following clearing. While this value is consistent with earlier predictions, water salvage may be short-lived

Table I. Summary of drought severity, annual ET (cm yr^{-1}), temperature extremes, total leaf area index (LAI_{Total}), and groundwater depth. Average annual Palmer drought severity index (PDSI) scores are the average monthly values from New Mexico regions 2 (North-central New Mexico) and 5 (Middle Rio Grande) (http://www.ncdc.noaa.gov/oa/climate/onlineprod/drought/xmgrg3.html). More negative PDSI values indicate increasingly severe drought. Average daily temperature extremes, both nighttime low (T_{min}) and the daytime high (T_{max}), were calculated as an average of the same 92 days in each year: 14–23 May, 13–16 June, 21 June–2 July, 11–12 July, 10–15 August, and 1 September–28 October. Maximum daily average groundwater depth (Gw_{max}) was measured from a well within 5 m of each tower

Site	Year: / PDSI:	2000 −0·04	2001 1·01	2002 −3·39	2003 −3·94	2004 −0·09
	ET (cm/yr):	134	125	127	125	114
Albuquerque	T_{min}/T_{max}	12·3/26·5	12·0/27·1	12·1/26·5	12·9/27·4	12·1/26·0
Populus deltoides[a]	LAI_{Total}	6·6 ± 0·2	7·0 ± 0·2	6·4 ± 0·2	4·0 ± 0·2	—
	Gw_{max} (cm)	(171)	(175)	(178)	(190)	(186)
	ET (cm/yr):	103	107	95	126	—
Belen	T_{min}/T_{max}	12·4/27·2	11·2/27·9	11·7/27·5	12·2/28·9	—
Populus deltoides	LAI_{Total}	5·0 ± 0·2	6·4 ± 0·2	6·0 ± 0·2	5·2 ± 0·2	—
	Gw_{max} (cm)	(118)	(139)	(155)	(168)	(163)
	ET (cm/yr):	86	83	71	69	80
Sevilleta NWR	T_{min}/T_{max}	10·1/28·6	8·8/29·5	9·2/28·5	9·8/29·6	8·6/27·8
Tamarix chinensis[b]	LAI_{Total}	3·5 ± 0·1	1·6 ± 0·2	0·9 ± 0·1	1·6 ± 0·2	—
	Gw_{max} (cm)	(213)	(218)	(227)	(245)	(240)
	ET (cm/yr):	118	115	87	101	114
Bosque del Apache NWR	T_{min}/T_{max}	9·7/28·6	7·8/29·2	9·2/29·4	9·3/30·4	9·0/28·1
Tamarix chinensis	LAI_{Total}	4·7 ± 0·1	5·0 ± 0·1	2·5 ± 0·1	4·1 ± 0·1	—
	Gw_{max} (cm)	(267)	(288)	(347)	(385)	(376)<

[a] Dense non-native understory removed during winter 2003/2004.
[b] Mosaic with *Distchlis spicata, Prosopis pubescens*, and *Atriplex* spp.

DOI: 10.1002/hyp

because *Tamarix* and *E. angustifolia* were allowed to regenerate during the 2005 growing season (data not shown) (Shafroth *et al*., 2005). Greater reduction in ET is expected to follow from converting a monospecific saltcedar stand (e.g. BDA NWR) into a saltgrass or meadow (Shafroth *et al*., 2005).

Recurrent, extended drought in the south-western United States, also referred to as 'megadrought,' is characterized by decreased regional precipitation in both the winter and summer modes. Recently, research has shown long-term sea-surface temperature anomalies to be related to these megadroughts, in which the Pacific decadal oscillation (PDO−) is in a cool phase and the Atlantic multi-decadal oscillation is in a warm phase (AMO+) (Gray *et al*., 2003). Resultant decline of regional precipitation and snowpack is initially ameliorated in the riparian corridor by release from reservoir storage, maintaining surface flow and groundwater resources. Along the MRG, droughts have recurred every 20–70 years (Gray *et al*., 2003).

Drought is expected to have an important recurring effect upon the MRG water budget, especially in naturally occurring processes like ET from riparian vegetation. Reduction in ET from *P. deltoides* stands was minimal, even during extreme drought (Table I). The vegetation did not experience the full intensity of what has been considered a major drought because municipal wastewater maintained the water table within 2 m of the surface at the Albuquerque site (Table I and Figure 2). Likewise, groundwater dynamics follow a hydrograph of irrigation operations rather than a natural flow regime at the Belen site (data not shown). Flow in the riverside drain maintained the water table at that site (Table I). As long as the irrigation and wastewater treatment systems are in operation, ET depletions from *P. deltoides* forests remain undiminished (Table I).

Evapotranspiration and LAI declined in the *Tamarix* sites during drought (Table I). Evapotranspiration at the Sevilleta NWR's *Tamarix* and *D. spicata* woodland tracked drought severity index values closely (Table I). BDA NWR's monospecific *Tamarix* thicket initially followed this trend, but ET and LAI began returning to pre-drought levels one year early, in 2003 (Table I). Groundwater levels also declined with drought at the *Tamarix* sites, especially during the late summer (Table I and Figure 2). Groundwater levels and annual variability had not begun to return to pre-drought patterns in 2004, the first year following relief from meteorological drought (Table I and Figure 2).

ET is often modelled as a function of groundwater depth (McDonald and Harbaugh, 1988). In the earliest conceptualization of this relationship, an elevation was defined above which ET is not limited by groundwater availability (i.e. $ET_{surface}$). At some deeper elevation, ET drops to zero because the water table is too deep

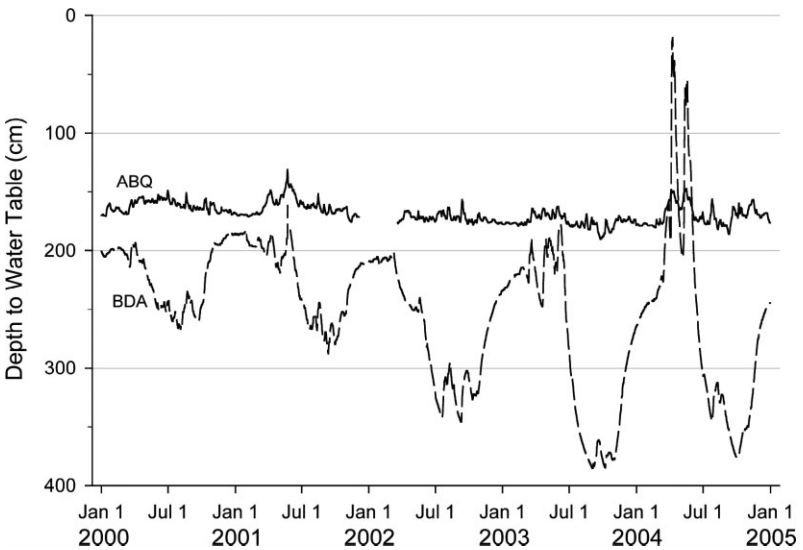

Figure 2. Daily average depth to groundwater (cm) in Albuquerque's south valley (ABQ) and at Bosque del Apache NWR (BdA). Pressure transducer measurements were logged once every 30 min from within 5 m of the tower

DOI: 10.1002/hyp

for roots to access (i.e. $ET_{extinction}$). Surface and extinction elevations are species specific. In *P. deltoides*, for example, these depths are $ET_{surface} = 3$ m and $ET_{extinction} = 5$ m (Horton *et al*., 2001). In fact, *P. deltoides* is well known for intolerance to groundwater recession, and crown dieback has been observed when the water table falls below 3 m (Stromberg *et al*., 1996; Scott *et al*., 1999; Rood *et al*., 2000; Cooper *et al*., 2003a). *P. deltoides*-dominated forests are typically found in places with a shallow and stable water table (Table I and Figure 2).

While $ET_{surface}$ and $ET_{extinction}$ are well defined in *P. deltoides*, depth to groundwater has not been found to restrict *Tamarix* ET, even when the water table is 10 m (Horton *et al*., 2001) or 25 m (Gries *et al*., 2003) below the surface. In the latter study, water storage in sand dunes sustained transpiration because *Tamarix* is a facultative phreatophyte capable of exploiting soil water in addition to groundwater (Busch *et al*., 1992; Smith *et al*., 1998). *Tamarix* tend to occupy sites with groundwater depth variability (Lite and Stromberg, 2005), and that is true at Bosque del Apache NWR where water table fluctuates more than 350 cm per year (Figure 2).

Water table depth was deepest in *Tamarix*-dominated sites (Table I). In 2003, the water table at BDA NWR fell below 3·5 m for the first time during the study (Figure 2). Groundwater decline was extreme that summer, falling as rapidly as 7 cm day^{-1} (Figure 3), from 175 cm below surface in May to 360 cm in September (Figure 2). While crown dieback occurred in a nearby *P. deltoides* forest (data not shown), a resurgence in *Tamarix* ET accompanied groundwater recession (Table I and Figure 3). ET from this *Tamarix* thicket increased substantially within a few days following the initiation of groundwater decline. Recently, Naumburg *et al*. (2005) proposed a mechanism that explains this counterintuitive finding.

For species like *Tamarix* that are not susceptible to moderate soil drying (Pockman and Sperry, 2000), a receding water table can increase the volume of aerated soil near field capacity (Naumburg *et al*., 2005). Draining of the soil is slower than the potential root growth rates in *Tamarix*, and the partly drained soil can be easily exploited (Naumburg *et al*., 2005). The initial delay results from the time required for the capillary fringe of the original water table ($GW_0 = 175$ cm) to drain sufficiently to allow respiration and root growth below GW_0. Once this hypothetical taproot growth is initiated, water uptake by new root growth at depths greater than GW_0 is augmented by continued fine root functioning at GW_0. Fine roots at the previous capillary fringe continue to function because *Tamarix*, unlike *P. deltoides*, is relatively tolerant of low xylem water potential (Pockman and Sperry, 2000).

A few days before 1 July, ET decreased and groundwater recession slowed (Figure 3). Stand-level ET declined again at the end of the year, preceding the year's maximum water table depth (GW_{max}) (Figures 2 and 3). Decreased groundwater decline rate and ET near the beginning of July was caused by multi-day monsoon precipitation, during which net radiation and VPD were minimized (data not shown). When that system had passed, groundwater decline and enhanced ET returned (Figure 3).

Dependence upon the shallow aquifer may be related to phreatophytic status (Smith *et al*., 1998). Thicket forming *Tamarix* spp. in the western US are facultative phreatophyte using water of an isotopic ratio intermediate between groundwater and precipitation sources (Busch *et al*., 1992). In *Populus* spp. use of precipitation water sources is conditional upon access to groundwater; in locations with a deep water table or ephemeral access to a shallow water table, *Populus* spp. utilize both deep and shallow water sources (Stromberg and Patten, 1996; Snyder and Williams, 2000). Of the dominant species along the MRG, *E. angustifolia* (Russian olive) is extremely varied in the habitats in which it thrives, but little has been documented regarding distributions where the groundwater is more than a few meters below the surface (Katz and Shafroth, 2003).

Average high and low temperature varied only slightly during the period between 2000 and 2004 (Table I). The southern sites experience hotter days and colder nights than the northern sites (Table I). This unusual pattern of minimum temperatures decreasing downstream can be explained by considering the distinct topographic features surrounding each site (Papadopoulos and Helmis, 1999). Katabatic winds, better known as cold air drainage, tend to be greatest in gullies and in mountainous terrain (Papadopoulos and Helmis, 1999; Soler *et al*., 2001). These mountainous hillsides have slopes that increase in angle from the valley floor

DOI: 10.1002/hyp

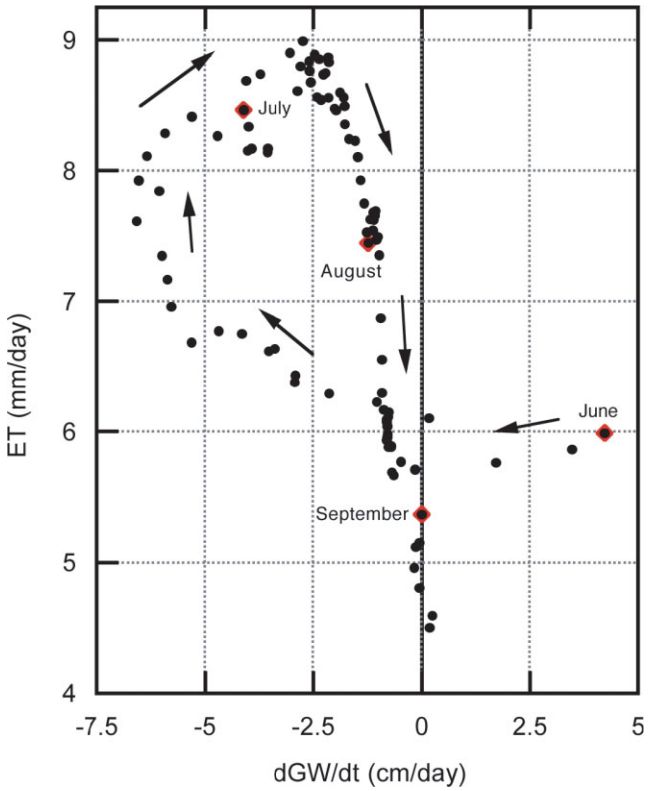

Figure 3. Temporal pattern of mean changes in groundwater depth and mean *T. chinensis* evapotranspiration in 2003 at Bosque del Apache National Wildlife Refuge. Change in groundwater depth is the difference between mean water table depth between two consecutive days, $dGW/dt = GW_{t-1} - GW_t$, where t is a discrete day. Negative values indicate a falling water table. Groundwater depth change and ET were smoothed with a 9-day running average. Refer to Figure 2 for daily depth to water table. The first day of each month is identified by a square, and arrows follow the progression of the growing season

to mountain peaks. Because sunrise does not illuminate the entire east-facing slope at once, an inversion layer is formed just below the sunrise line. Katabatic flow continues below this inversion layer and anabatic flow begins above (Papadopoulos and Helmis, 1999). Because of the mountainous terrain near the downstream reaches of the MRG, cold air drainage into the *Tamarix* thickets maintains colder nighttime temperature (Table I).

FLOODING AND MICRO-METEOROLOGY (RAPID DYNAMICS)

Limited flooding of two sites, Belen–Rio Communities and BDA NWR, occurred during spring 2001 owing to a 1-day water release of 115 $m^3\ s^{-1}$ from Cochiti Reservoir by the US Army Corps of Engineers (Figure 4). The travel time of this flood pulse was 48 h between these two sites (Figure 4). At BDA, floodwater flowed into the floodplain over the bank 0·5–1 km upstream of the tower. Surface flow travelled parallel to the river, in contrast to flooding near Rio Communities, where stagnant open water arose from seepage. Surface inundation was short-lived at both sites, and the water table peaked for a single day (Figure 4).

During onsite flooding, groundwater levels in the monitoring wells failed to reach the surface at either flooded site. At the northern cottonwood-dominated site, the water table reached the surface in some locations but not in others, averaging 55 cm below the average land surface (Figure 4). Local topographical relief is

DOI: 10.1002/hyp

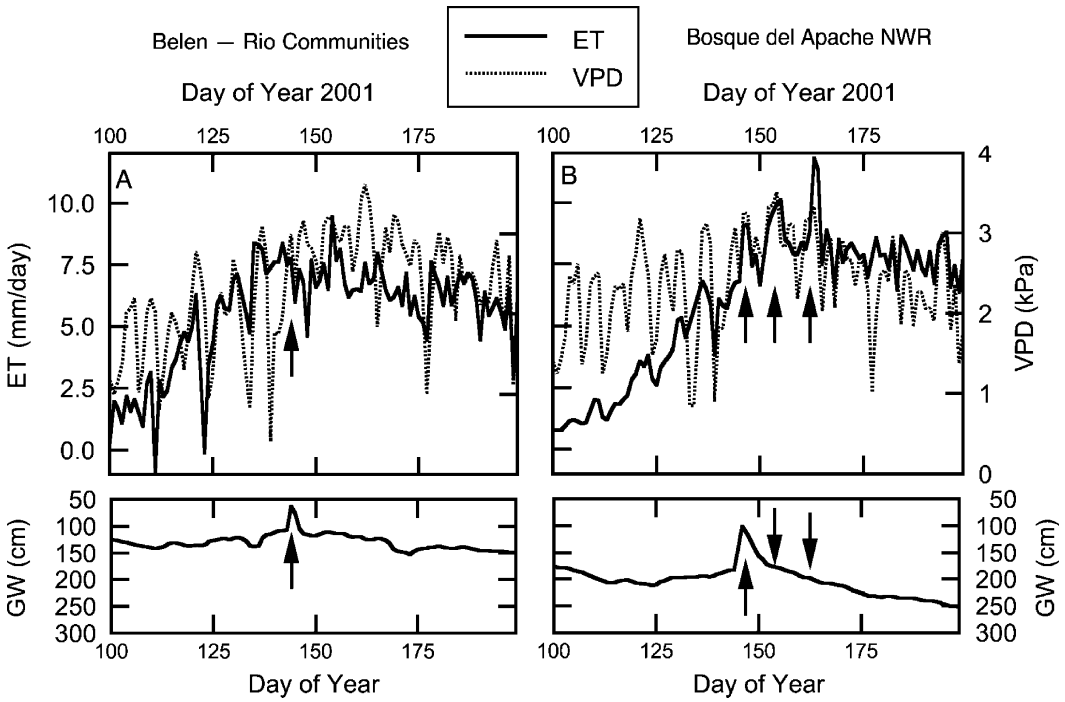

Figure 4. Time series of daily evapotranspiration (ET), vapour pressure deficit (VPD), and depth to groundwater. Floodwaters were present at the Belen–Rio Communities *P. deltoides* ssp. *wislizeni* (A) and Bosque del Apache *Tamarix s* (B) sites on 24 May and 26 May 2001, respectively. The arrows in panel A and the first pair of arrows in panel B point to the day of inundation. The two following pairs of arrows in panel B point to days following ET maxima

50 cm between the highest- and lowest-lying wells, but these wells represent only a fraction of the total topographic relief. Surface flooding was likewise observed in depressions but not ridges within the active floodplain.

Total ET from this *P. deltoides* forest did not increase during or following inundation (Figure 4). Net radiation reaching the forest floor through the canopy is minimal, generally between 50 and 100 W m^{-2}, providing little energy for forest floor evaporation (Wilson *et al.*, 2001). At the same time, transpiration is not curtailed completely due to root hypoxia, for only a fraction of the active roots are likely to be under the water table.

Flooding in the monospecific *Tamarix* thicket was associated with elevated total ET rates (Figure 4). Unlike the loamy sand underlying the *P. deltoides* forest, the soil at this site is dominated by loamy clay. The Rio Puerco is well known for generating a load of very fine sediments into the MRG (Phippen and Wohl, 2003; Gellis *et al.*, 2004). Fine sediments defloculate when wetted, creating an infiltration barrier. Therefore, the top meter of soil did not reach field capacity even though surface water was observed around all groundwater wells (Figure 4).

Stepwise multiple regression tests of ET and variable suites (Table II), ET rates were found to be closely coupled to VPD at the *Tamarix* sites (Table III and Figure 4). *Tamarix*' cylindrical leaves form a minimal boundary layer, and stomata respond rapidly to atmospheric conditions and thereby closely link transpiration to micro-meteorological conditions (Table III) (Jarvis and McNaughton, 1986; Hollinger *et al.*, 1994; Meinzer *et al.*, 1997; Nagler *et al.*, 2005a). At the *P. deltoides* sites, coupling between VPD and ET was observed for a part of the year, but asynchrony between VPD and ET fluctuations was observed during flooding (Figure 4). On average, short-term fluctuations in *P. deltoides* ET were not closely coupled to fluctuations in VPD (Table III).

DOI: 10.1002/hyp

Table II. Variables evaluated in stepwise multiple regression. During each iteration, variables with a probability of a type II error > 0·1 ($p > 0{\cdot}1$) was removed from the analysis

Variable	Units	Definition
Energy Balance:		
R_n	W m^{-2}	Daytime Net Radiation
H	W m^{-2}	Sensible Heat Flux
G	W m^{-2}	Ground Heat Flux
Aerodynamics:		
u	m s^{-1}	Daytime Windspeed along riparian corridor
v	m s^{-1}	Daytime Windspeed across (i.e. tangential to) riparian corridor
ws	m s^{-1}	Daytime 2-D Horizontal windspeed
nu	m s^{-1}	Nighttime windspeed along riparian corridor
nv	m s^{-1}	Nighttime windspeed across riparian corridor
nws	m s^{-1}	Nighttime 2-D Horizontal windspeed
u_*	m s^{-1}	Friction coefficient or velocity
q_*	g_{water} $g_{air}{}^{-1}$	Humidity scale in the surface layer
L	m	Obukhov Length
Meteorological Conditions:		
GDD	°C	Growing Degree Days
PPT	mm day^{-1}	Precipitation
q	g_{water} $g_{air}{}^{-1}$	Specific Humidity
T_{max}	°C	Daily High Temperature
T_{min}	°C	Daily Low Temperature
T	°C	Daily Average Temperature
VPD	kPa	Vapour pressure deficit
P	kPa	Atmospheric Pressure
Other:		
GW	cm	Depth to groundwater

Coupling between ET and atmospheric conditions was closer at the *Tamarix* sites than at the *P. deltoides* sites (Table III and Figure 5). Evapotranspiration (ET) from the *Tamarix* canopy was especially sensitive to aerodynamic characteristics of the surface layer (Table III). Variations in u_* are observed under advection, when temperature inversions within the lower atmosphere constrain the extent of the surface layer (Cooper *et al*., 2003b).

Precipitation decreases ET and H at the *Tamarix* sites through shading and the resulting reduction in R_n (Table III). Because vegetation along the MRG are not water limited owing to the close proximity of groundwater (Table I and Figure 2), precipitation does not directly lead to changes in ET (Table III), in contrast to the flush of leaf gas exchange that follows precipitation in drier riparian habitats (Huxman *et al*., 2004). The interaction of daily temperature extremes also contributed to the micro-meteorological control of *Tamarix* ET (Tables I and III) (Nagler *et al*., 2005a).

Energy balance and horizontal wind direction explained slightly more than 50% of the daily variability in *P. deltoides* ET (Table III and Figure 5). Sensible heat advection, carried on the wind tangential to the riparian corridor, and the development of a thick local boundary layer, reduces the coupling among stomatal conductance, vapour pressure deficit, and transpiration (Table III) (Jarvis and McNaughton, 1986). Sensible heat advection and surface layer dynamics had a stronger effect on *P. deltoides* ET in Albuquerque's south valley than in Belen (data not shown).

Modelled ET anomalies fit well with measured anomalies, especially at the *Tamarix* sites (Figure 5). Residuals from the regression analysis were evenly distributed around the model line (Figure 5), suggesting

DOI: 10.1002/hyp

Table III. Results of stepwise multiple regression model between evapotranspiration anomalies and micro-meteorological conditions. ET anomalies were identified when daily ET was more than one standard deviation above or below the 9-day running average. For ease of interpretation, factors related to ET anomalies are separated into energy, aerodynamic, and meteorological conditions. See text and Table II for descriptions of the modelled dependent variables. Models for predicting ET anomalies are $[ET_{anomaly} = -0{\cdot}008\,H + 0{\cdot}02\,R_n - 0{\cdot}1\,v - 0{\cdot}09(v \times u)]$ ($r^2 = 0{\cdot}54$) in cottonwood forests and $[ET_{anomaly} = 0{\cdot}005\,R_n + 0{\cdot}08\,u + 1{\cdot}2\,u_* - 4{\cdot}2\,q_* + 11{\cdot}8\,(u_* \times q_*) - 0{\cdot}5\,VPD - 0{\cdot}01\,(T_{max} \times T_{min}) - 0{\cdot}003(PPT \times H) + 0{\cdot}001\,(R_n \times PPT)]$ ($r^2 = 0{\cdot}66$) for saltcedar stands

Factor	Coefficient ± se	F	p
	Albuquerque and Belen–Rio Communities, *Populus deltoides*		
Model:	**0·54**	**110.8**	**<0.0001**
Energy Balance:			
H	−0·008 ± 0·002	19·2	<0·0001
R_n	0·02 ± 0·0008	388·1	<0·0001
Aerodynamics:			
v	−0·1 ± 0·06	5·8	0·02
$v \times u$	−0·09 ± 0·02	16·2	<0·0001
	Sevilleta and Bosque del Apache NWRs, *Tamarix chinensis*		
Model:	**0·66**	**77.7**	**<0.0001**
Energy Balance:			
R_n	0·005 ± 0·0005	83·7	<0·0001
Aerodynamics:			
u	0·08 ± 0·03	7·5	0·007
u_*	1·2 ± 0·3	12·9	0·0004
q_*	−4·2 ± 0·6	50·2	<0·0001
$u_* \times q_*$	11·8 ± 4·3	7·4	0·007
Meteorological Conditions:			
VPD	0·5 ± 0·07	43·0	<0·0001
$T_{max} \times T_{min}$	−0·01 ± 0·003	9·8	0·002
Interacting Effects:			
PPT × H	—0·003 ± 0·0005	24·3	<0·0001
R_n × PPT	0·001 ± 0·0003	18·4	<0·0001

that the anomaly dataset is essentially free from autocorrelation bias (Nagler *et al*., 2005a). For the most part, energy balance and aerodynamics are related to short-term fluctuations in riparian ET (Table III) (Pieri and Fuchs, 1990). Variables that were included in the analysis, but which did not show any relationship to ET fluctuations, included depth to groundwater, G, and barometric pressure (Tables II and III). Ground heat flux is near zero and does not vary (data not shown). Depth to groundwater does vary, but at a slower scale that could not be detected in the short-term analysis.

CONCLUSIONS

Evapotranspiration rates were compared among native and non-native riparian vegetation along the MRG in New Mexico. Evapotranspiration from xeroriparian shrubs, including non-native *Tamarix* and native *D. spicata*, was lower than ET from any other vegetation class (Table I). Highest ET rates were measured

DOI: 10.1002/hyp

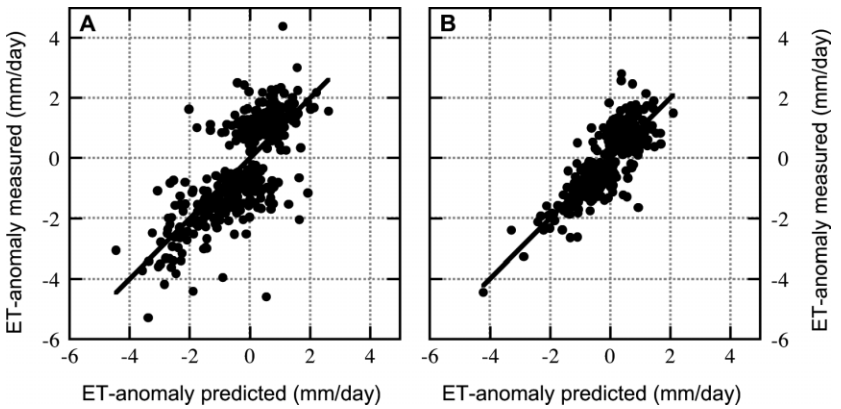

Figure 5. Measured and predicted evapotranspiration anomalies at the Populus deltoides (A) and Tamarix chinensis (B) sites. Predicted anomalies were defined as the solution to the best-fit stepwise multiple linear regression model (Table III)

from a multi-layered canopy site in which non-native *Tamarix* and *E. angustifolia* formed a thick understory with a *P. deltoides* forest (Table I). However, the monospecific *Tamarix* and native *P. deltoides* forest without a dense non-native understory also support ET rates greater than 100 cm yr^{-1}, which is three to five times the annual precipitation in the basin (Table I) (Dahm *et al*., 2002). Energy balance closure was 78%, well within the 10–30% error range for eddy covariance systems (Twine *et al*., 2000).

Reduction in ET following removal of the non-native understory from a *P. deltoides* canopy resulted in a modest 21% reduction in ET relative to the reference sites (Table I) (Shafroth *et al*., 2005). However, ET at the post-removal site was lower than it had been in any other year at that site, it was the first year that this site did not support higher ET rates compared to any other site. Water salvage will be transitory, however, should the non-native understory be allowed to regenerate. To be economically feasible, an emphasis on long-term success in restoration projects needs to be pursued.

ET rates respond to groundwater depth, stomatal coupling to atmospheric humidity, leaf area index, atmospheric surface layer conditions, and energy balance. The recent severe drought had little effect on native *P. deltoides* forests because water tables were artificially maintained to within 2 m of the surface, but *Tamarix* water use and LAI were diminished under drought conditions (Table I). However, water table decline during drought resulted in 50% higher ET rates from a dense, monospecific *Tamarix* thicket (Figure 3). ET from *Tamarix* is closely coupled to atmospheric conditions rather than water table depth (Table III and Figure 4). ET from *P. deltoides* is responsive to variations in energy balance and sensible heat advection rather than atmospheric humidity or temperature (Table III) (Horton *et al*., 2001).

ACKNOWLEDGEMENTS

The authors would like to thank Laurence Hipps, John Prueger, Daniel Cooper, and Salim Bawazir for their conceptual, computational, and methodological assistance. We would like to further thank the Society of Range Management for sponsoring the symposium that lead to the preparation of this paper. Site access was granted by the Sevilleta NWR, Bosque del Apache NWR, La Joya State Game Refuge, the Middle Rio Grande Conservancy District, New Mexico's state forestry department, and the city of Albuquerque's open space division. Further thanks for their ongoing interest are offered to the Hydrogeoecology and the Sevilleta Long Term Ecological Research groups at the University of New Mexico, the New Mexico interagency ET workgroup, the Bosque Hydrology Group, and the New Mexico State EPSCoR office. This research has been funded by NASA award NAG5-6999, the New Mexico Interstate Stream Commission, the US Fish and Wildlife Service's Bosque Initiative, the US Bureau of Reclamation's Endangered Species Workgroup, and a

DOI: 10.1002/hyp

NSF-EPSCoR Research Infrastructure Improvement award. We would finally like to thank three anonymous reviewers for their assistance in improving an early version of this manuscript.

REFERENCES

Brunet Y, Itier B, McAneney J, Lagouarde JP. 1994. Downwind evolution of scalar fluxes and surface resistance under conditions of local advection. Part II: measurements over barley. *Agricultural and Forest Meteorology* **71**: 227–245.

Busch DE, Smith SD. 1993. Effects of fire on water and salinity relations of riparian woody taxa. *Oecologia* **94**: 186–194.

Busch DE, Smith SD. 1995. Mechanisms associated with decline of woody species in riparian ecosystems of the southwestern U.S. *Ecological Monographs* **65**: 347–370.

Busch DE, Ingraham NL, Smith SD. 1992. Water uptake in woody riparian phreatophytes of the Southwestern United States: a stable isotope study. *Ecological Applications* **2**: 450–459.

Campbell CJ, Dick-Peddie WA. 1964. Comparison of phreatophytic communities on the Rio Grande in New Mexico. *Ecology* **45**: 492–502.

Chen JM, Black TA. 1992. Defining leaf-area index for non-flat leaves. *Plant Cell and Environment* **15**: 421–429.

Chen JM, Cihlar J. 1995. Quantifying the effect of canopy architecture on optical measurements of leaf-area index using 2 gap size analysis-methods. *IEEE Transactions On Geoscience and Remote Sensing* **33**: 777–787.

Chen JM, Cihlar J. 1996. Retrieving leaf area index of boreal conifer forests using landsat TM images. *Remote Sensing of Environment* **55**: 153–162.

Cleverly JR, Smith SD, Sala A, Devitt DA. 1997. Invasive capacity of *Tamarix ramosissima* in a Mojave Desert floodplain: the role of drought. *Oecologia* **111**: 12–18.

Cleverly JR, Dahm CN, Thibault JR, Gilroy DJ, Coonrod JEA. 2002. Seasonal estimates of actual evapo-transpiration from *Tamarix ramosissima* stands using three-dimensional eddy covariance. *Journal of Arid Environments* **52**: 181–197.

Cooper D, D'Amico D, Scott M. 2003a. Physiological and morphological response patterns of *Populus deltoides* to alluvial groundwater pumping. *Environmental Management* **31**: 215–226. Doi: 10·1007/s00267-002-2808-2.

Cooper D, Eichinger W, Archuleta J, Hipps L, Kao J, Leclerc M, Neale C, Prueger J. 2003b. Spatial source-area analysis of three-dimensional moisture fields from LIDAR, eddy covariance, and a footprint model. *Agricultural and Forest Meteorology* **114**: 213–234.

Cooper DI, Eichinger WE, Kao J, Hipps L, Reisner J, Smith S, Schaeffer SM, Williams DG. 2000. Spatial and temporal properties of water vapour and latent energy flux over a riparian canopy. *Agricultural and Forest Meteorology* **105**: 161–183.

Dahm CN, Cleverly JR, Coonrod JEA, Thibault JR, McDonnell DE, Gilroy DF. 2002. Evapotranspiration at the land/water interface in a semi-arid drainage basin. *Freshwater Biology* **47**: 831–843.

Devitt DA, Sala A, Smith SD, Cleverly J, Shaulis LK, Hammett R. 1998. Bowen ratio estimates of evapotranspiration for *Tamarix ramosissima* stands on the Virgin River in southern Nevada. *Water Resources Research* **34**: 2407–2414.

Di Tomaso J. 1998. Impact, biology, and ecology of saltcedar (Tamarix spp.) in the southwestern United States. *Weed Technology* **12**: 326–336.

Drexler JZ, Snyder RL, Spano D, Paw UKT. 2004. A review of models and micrometeorological methods used to estimate wetland evapotranspiration. *Hydrological Processes* **18**: 2071–2101. Doi: 10.1002/hyp.1462.

Everitt B. 1998. Chronology of the spread of tamarisk in the central Rio Grande. *Wetlands* **18**: 658–668.

Friedman JM, Auble GT, Shafroth PB, Scott ML, Merigliano MF, Preehling MD, Griffin EK. 2005. Dominance of non-native riparian trees in western USA. *Biological Invasions* **7**: 747–751.

Gay LW, Fritschen LJ. 1979. An energy budget analysis of water use by saltcedar. *Water Resources Research* **15**: 1589–1592.

Gellis AC, Pavich MJ, Bierman PR, Clapp EM, Ellevein A, Aby S. 2004. Modern sediment yield compared to geologic rates of sediment production in a semi-arid basin, New Mexico: assessing the human impact. *Earth Surface Processes and Landforms* **29**: 1359–1372.

Goodrich DC, Scott R, Qi J, Goff B, Unkrich CL, Moran MS, Williams D, Schaeffer S, Snyder K, MacNish R, Maddock T, Pool D, Chehbouni A, Cooper DI, Eichinger WE, Shuttleworth WJ, Kerr Y, Marsett R, Ni W. 2000. Seasonal estimates of riparian evapotranspiration using remote and in situ measurements. *Agricultural and Forest Meteorology* **105**: 281–309.

Gower ST, Norman JM. 1991. Rapid estimation of leaf-area index in conifer and broad-leaf plantations. *Ecology* **72**: 1896–1900.

Gray S, Betancourt J, Fastie C, Jackson S. 2003. Patterns and sources of multidecadal oscillations in drought-sensitive tree-ring records from the central and southern Rocky Mountains. *Geophysical Research Letters* **30**: 1316.

Gries D, Zeng F, Foetzki A, Arndt S, Bruelheide H, Thomas F, Zhang X, Runge M. 2003. Growth and water relations of *Tamarix ramosissima* and *Populus euphratica* on Taklamakan desert dunes in relation to depth to a permanent water table. *Plant Cell and Environment* **26**: 725–736.

Higgins RW, Yao Y, Wang XL. 1997. Influence of the North American monsoon system on the US summer precipitation regime. *Journal of Climate* **10**: 2600–2622.

Hollinger DY, Kelliher FM, Schulze E-D, Köstner BMM. 1994. Coupling of tree transpiration to atmospheric turbulence. *Nature* **371**: 60–62.

Horton JL, Kolb TE, Hart SC. 2001. Physiological response to groundwater depth varies among species and with river flow regulation. *Ecological Applications* **11**: 1046–1059.

Howe CD, Chancellor RJ. 1983. Factors affecting the viable seed content of soils beneath lowland pastures. *Journal of Applied Ecology* **20**: 915–922.

Howe WH, Knopf FL. 1991. On the imminent decline of Rio Grande cottonwoods in central New Mexico. *Southwestern Naturalist* **36**: 218–224.

Hughes LE. 1993. "The devil's own"–Tamarisk. *Rangelands* **15**: 151–155.

Huxman TE, Snyder KA, Tissue D, Leffler AJ, Ogle K, Pockman WT, Sandquist DR, Potts DL, Schwinning S. 2004. Precipitation pulses and carbon fluxes in semiarid and arid ecosystems. *Oecologia* **141**: 254–268.
Huxman TE, Wilcox BP, Breshears DD, Scott RL, Snyder KA, Small EE, Hultine K, Pockman WT, Jackson RB. 2005. Ecohydrological implications of woody plant encroachment. *Ecology* **86**: 308–319.
Itier B, Brunet Y, McAneney KJ, Lagouarde JP. 1994. Downwind evolution of scalar fluxes and surface resistance under conditions of local advection. Part I: a reappraisal of boundary conditions. *Agricultural and Forest Meteorology* **71**: 211–225.
Jackson RB, Carpenter SR, Dahm CN, McKnight DM, Naiman RJ, Postel SL, Running SW. 2001. Water in a changing world. *Ecological Applications* **11**: 1027–1045.
Jarvis PG, McNaughton KG. 1986. Stomatal control of transpiration: scaling up from leaf to region. *Advances in Ecological Research* **15**: 1–49.
Kao CYJ, Hang YH, Cooper DI, Eichinger WE, Smith WS, Reisner JM. 2000. High-resolution modelling of LIDAR data mechanisms governing surface water vapour variability during SALSA. *Agricultural and Forest Meteorology* **105**: 185–194.
Katz G, Shafroth P. 2003. Biology, ecology and management of *Elaeagnus angustifolia* L. (Russian olive) in western North America. *Wetlands* **23**: 763–777.
Kurc SA, Small EE. 2004. Dynamics of evapotranspiration in semiarid grassland and shrubland ecosystems during the summer monsoon season, central New Mexico. *Water Resources Research* **40**: W09305.
Lite SJ, Stromberg JC. 2005. Surface water and ground-water thresholds for maintaining Populus-Salix forests, San Pedro River, Arizona. *Biological Conservation* **125**: 153–167.
Malanson GP. 1995. *Riparian Landscapes*. Cambridge University Press: Cambridge.
Massman W. 2000. A simple method for estimating frequency response corrections for eddy covariance systems. *Agricultural and Forest Meteorology* **104**: 185–198.
Massman W. 2001. Reply to comment by Rannik on "A simple method for estimating frequency response corrections for eddy covariance systems". *Agricultural and Forest Meteorology* **107**: 247–251.
McAneney KJ, Brunet Y, Itier B. 1994. Downwind evolution of transpiration by two irrigated crops under conditions of local advection. *Journal of Hydrology* **161**: 375–388.
McDonald MG, Harbaugh AW. 1988. A modular three-dimensional finite-difference ground-water flow model. US Geological Survey, TWI 6-A1.
Medina AL. 1990. Possible effects of residential development on streamflow, riparian plant communities, and fisheries on small mountain streams in central Arizona. *Forest Ecology and Management* **33**: 1–4.
Meinzer FC, Hinckley TM, Ceulemans R. 1997. Apparent responses of stomata to transpiration and humidity in a hybrid poplar canopy. *Plant Cell and Environment* **20**: 1301–1308.
Molles MC, Crawford CS, Ellis LM, Valett HM, Dahm CN. 1998. Managed flooding for riparian ecosystem restoration: managed flooding reorganizes riparian forest ecosystems along the middle Rio Grande in New Mexico. *Bioscience* **48**: 749–756.
Nagler PL, Cleverly J, Glenn E, Lampkin D, Huete A, Wan ZM. 2005a. Predicting riparian evapotranspiration from MODIS vegetation indices and meteorological data. *Remote Sensing of Environment* **15**: 17–30.
Nagler PL, Hinojosa-Huerta O, Glenn EP, Garcia-Hernandez J, Romo R, Curtis C, Huete AR, Nelson SG. 2005b. Regeneration of native trees in the presence of invasive saltcedar in the Colorado River delta, Mexico. *Conservation Biology* **19**: 1842–1852.
Nakamura R, Mahrt L. 2001. Similarity theory for local and spatially averaged momentum fluxes. *Agricultural and Forest Meteorology* **108**: 265–279.
Naumburg E, Mata-Gonzalez R, Hunter RG, Mclendon T, Martin DW. 2005. Phreatophytic vegetation and groundwater fluctuations: a review of current research and application of ecosystem response modelling with an emphasis on Great Basin vegetation. *Environmental Management* **35**: 726–740.
Newman BD, Wilcox BP, Archer S, Breshears DD, Dahm CN, Duffy CJ, McDowell NG, Phillips FM, Scanlon BR, Vivoni ER. 2006. The ecohydrology of arid and semiarid environments: a scientific vision. *Water Resources Research* **42**: W06302. DOI:10.1029/2005WR004141.
Papadopoulos K, Helmis C. 1999. Evening and morning transition of katabatic flows. *Boundary-Layer Meteorology* **92**: 195–227.
Pataki DE, Bush SE, Gardner P, Solomon DK, Ehleringer JR. 2005. Ecohydrology in a Colorado River riparian forest: Implications for the decline of Populus fremontii. *Ecological Applications* **15**: 1009–1018.
Phippen SJ, Wohl E. 2003. An assessment of land use and other factors affecting sediment loads in the Rio Puerco watershed, New Mexico. *Geomorphology* **16**: 3–4.
Pieri P, Fuchs M. 1990. Comparison of Bowen Ration and aerodynamic estimates of evapotranspiration. *Agricultural and Forest Meteorology* **49**: 243–256.
Planty-Tabacchi A-M, Tabacchi E, Naiman RJ, Deferrari C, Decamps H. 1996. Invasibility of species-rich communities in riparian zones. *Conservation Biology* **10**: 598–607.
Pockman W, Sperry J. 2000. Vulnerability to xylem cavitation and the distribution of Sonoran desert vegetation. *American Journal of Botany* **87**: 1287–1299.
Rannik U, Aubinet M, Kurbanmuradov O, Sabelfeld K, Markkanen T, Vesala T. 2000. Footprint analysis for measurements over a heterogeneous forest. *Boundary-Layer Meteorology* **97**: 137–166.
Rood S, Patino S, Coombs K, Tyree M. 2000. Branch sacrifice: cavitation-associated drought adaptation of riparian cottonwoods. *Trees-Structure And Function* **14**: 248–257.
Sala A, Devitt DA, Smith SD. 1996. Water use by *Tamarix ramosissima* and associated phreatophytes in a Mojave Desert floodplain. *Ecological Applications* **6**: 888–898.
Saugier B, Katerji N. 1991. Some plant factors controlling evapotranspiration. *Agricultural and Forest Meteorology* **54**: 263–277.
Scott ML, Shafroth PB, Auble GT. 1999. Responses of riparian cottonwoods to alluvial water table declines. *Environmental Management* **23**: 347–358.

Scott RL, Shuttleworth WJ, Goodrich DC, Maddock T. 2000. The water use of two dominant vegetation communities in a semiarid riparian ecosystem. *Agricultural and Forest Meteorology* **105**: 241–256.
Scott RL, Watts C, Payan JG, Edwards E, Goodrich DC, Williams D, Shuttleworth WJ. 2003. The understory and overstory partitioning of energy and water fluxes in an open canopy, semiarid woodland. *Agricultural and Forest Meteorology* **114**: 127–139.
Shafroth PB, Cleverly JR, Dudley TL, Taylor JP, Van Riper C, Weeks EP, Stuart JN. 2005. Control of *Tamarix* in the Western United States: implications for water salvage, wildlife use, and riparian restoration. *Environmental Management* **35**: 231–246.
Simpson IJ, Thurtell GW, Neumann HH, Den Hartog G, Edwards GC. 1998. The validity of similarity theory in the roughness sublayer above forests. *Boundary-Layer Meteorology* **87**: 69–99.
Smith SD, Wellington AB, Nachlinger JL, Fox CA. 1991. Functional responses of riparian vegetation to streamflow diversion in the eastern Sierra Nevada. *Ecological Applications* **1**: 89–97.
Smith SD, Devitt DA, Sala A, Cleverly JR, Busch DE. 1998. Water relations of riparian plants from warm desert regions. *Wetlands* **18**: 687–696.
Snyder WD, Miller GC. 1993. Changes in riparian vegetation along the Colorado River and Rio Grande, Colorado. *Great Basin Naturalist* **52**: 357–363.
Snyder K, Williams D. 2000. Water sources used by riparian trees varies among stream types on the San Pedro River, Arizona. *Agricultural and Forest Meteorology* **105**: 227–240.
Soler M, Infante C, Buenestado P, Mahrt L. 2001. Observations of nocturnal drainage flow in a shallow gully. *Boundary-Layer Meteorology* **105**: 253–273.
Stromberg J, Patten D. 1996. Instream flow and cottonwood growth in the eastern Sierra Nevada of California, USA. *Regulate Rivers: Research and Management* **12**: 1–12.
Stromberg JC, Tiller R, Richter B. 1996. Effects of groundwater decline on riparian vegetation of semiarid regions: the San Pedro, Arizona. *Ecological Applications* **6**: 113–131.
Stull RB. 1988. *An Introduction to Boundary Layer Meteorology*. Kluwer Academic Publishers: Boston, MA.
Tiegs SD, O'Leary JF, Pohl MM, Munill CL. 2005. Flood disturbance and riparian species diversity on the Colorado River Delta. *Biodiversity and Conservation* **14**: 1175–1194.
Twine TE, Kustas WP, Norman JM, Cook DR, Houser PR, Meyers TP, Prueger JH, Starks PJ, Wesely ML. 2000. Correcting eddy-covariance flux underestimates over a grassland. *Agricultural and Forest Meteorology* **103**: 279–300.
Warren DK, Turner RM. 1975. Saltcedar (Tamarix chinesis) seed production, seedling establishment, and response to inundation. *Journal of the Arizona Academy of Sciences* **10**: 135–144.
Webb E, Pearman G, Leuning R. 1980. Correction of flux measurements for density effects due to heat and water-vapour transfer. *Quarterly Journal of the Royal Meteorological Society* **106**: 85–100.
Wesely ML. 1970. *Eddy correlation measurements in the atmospheric surface layer over agricultural crops*. PhD Dissertation, University of Wisconsin, Madison, UI; 102.
Wilson K, Baldocchi D, Aubinet M, Berbigier P, Bernhofer C, Dolman H, Falge E, Field C, Goldstein A, Granier A, Grelle A, Halldor T, Hollinger D, Katul G, Law B, Lindroth A, Meyers T, Moncrieff J, Monson R, Oechel W, Tenhunen J, Valentini R, Verma S, Vesala T, Wofsy S. 2002. Energy partitioning between latent and sensible heat flux during the warm season at FLUXNET sites. *Water Resources Research* **38**: 1294. Doi: 10·1029/2001WR000989.
Wilson K, Hanson P, Mulholland P, Baldocchi D, Wullschleger S. 2001. A comparison of methods for determining forest evapotranspiration and its components: sap-flow, soil water budget, eddy covariance and catchment water balance. *Agricultural and Forest Meteorology* **106**: 153–168.
Zube EH, Simcox DE. 1987. Arid lands, riparian landscapes, and management conflicts. *Environmental Management* **11**: 529–535.

DOI: 10.1002/hyp